

# Plasmon surface waves and complex-type surface waves: comparative analysis of single interfaces, lamellar gratings, and two-dimensional hole arrays

Evgeny Popov, Stefan Enoch, and Michel Nevière

The similarities and differences between two types of surface waves that can exist on a plane metal-lossless dielectric interface, on the one hand, and on a plane lossy-lossless dielectric interface, on the other hand, are analyzed numerically. They both can lead to total absorption of light by surface relief gratings and show different behavior in transmission by lamellar gratings. © 2007 Optical Society of America

OCIS codes: 050.1950, 050.1960.

## 1. Introduction

Metallic gratings have been well known since the dawn of the 20th century<sup>1</sup> to present resonance anomalies. They are commonly due to excitation of plasmon surface waves that can propagate on a single metallic-dielectric interface in TM polarization (magnetic field vector perpendicular to the plane of incidence). After the work of Ebbesen *et al.*,<sup>2</sup> numerous studies have been devoted to two-dimensional gratings consisting of arrays of periodically arranged holes in metallic screens that exhibit enhanced transmission due to surface plasmon excitation, a phenomenon having already found many applications in physics and biology.<sup>3</sup>

There exist several other types of resonant anomalies, due to excitation of cavity resonances<sup>4</sup> or waveguide modes,<sup>5</sup> in both TE and TM polarization. Recently, another type of surface wave<sup>6</sup> has been found responsible for grating anomalies in cases when the grating material represents a lossy dielectric with large values of real and imaginary parts of the relative electric permittivity  $\epsilon_d$ . The common features with the plasmon surface wave are that this surface wave, called the complex surface wave,<sup>7</sup> ex-

ists on a single plane interface in TM polarization and that its propagating constant  $k_x$  along the surface is subjected to the same condition as the plasmon surface wave. Namely, it represents a zero of the denominator of the Fresnel coefficients in reflection and transmission in TM polarization:

$$k_{1,y}/\epsilon_1 + k_{2,y}/\epsilon_2 = 0, \quad (1)$$

where  $\epsilon_1$  and  $\epsilon_2$  are the relative permittivities of the two media, and

$$k_{j,y} = \sqrt{\epsilon_0 \epsilon_j - k_x^2}, \quad j = 1, 2, \quad (2)$$

are the  $y$  components of the wave vectors in each medium, perpendicular to the interface, with  $\epsilon_0$  being the vacuum permittivity.

It is well known that the solution of Eq. (1) can be written in the form

$$k_x = k_0 \sqrt{\frac{\epsilon_1 \epsilon_2}{\epsilon_1 + \epsilon_2}}, \quad (3)$$

where  $k_0$  is the vacuum wavenumber.

Let us assume, without losing the generality, that the upper medium is vacuum, so that Eq. (3) is simplified and the normalized propagation constant can be written as

$$k_0/k_x = \sqrt{\frac{\epsilon_2}{1 + \epsilon_2}}. \quad (4)$$

The authors are with the Institut Fresnel, Domaine Universitaire de Saint Jérôme, Université de Provence, CNRS UMR 6133, 13397 Marseille Cedex 20, France. E. Popov's e-mail address is e.popov@fresnel.fr.

Received 7 July 2006; revised 22 September 2006; accepted 26 September 2006; posted 28 September 2006 (Doc. ID 72790); published 21 December 2006.

0003-6935/07/020154-07\$15.00/0

© 2007 Optical Society of America

For a lossless substrate, in order that this wave decay when moving away from the interface, it is necessary that  $\epsilon_2 < -1$ ; i.e., the substrate must be metallic. However, when real lossy materials are considered, the propagation constant becomes complex, as well as  $k_{1,y}$  and  $k_{2,y}$ . In that case, the condition for the surface wave to remain decaying is simply given by the relations  $\text{Im}(k_{1,y}) > 0$  and  $\text{Im}(k_{2,y}) > 0$ , assuming the  $y$  dependences are in the form  $\exp(ik_{1,y}y)$  and  $\exp(-ik_{2,y}y)$ . Such a solution can be supported by a real metal–dielectric interface, but also along the interface between two dielectrics, the decay of the field for  $y \rightarrow \pm\infty$  is ensured by the imaginary part of  $k_{j,y}$ ,  $j = 1, 2$ , existing due to the losses.

Both types of surface wave can be excited using a periodic corrugation of the surface. Our aim is to make a comparative study of grating anomalies due to them by using the differential method for modeling the diffraction by periodic structures.<sup>8</sup>

## 2. Plasmon Surface Wave and Complex Surface Wave along a Plane Interface

Despite the features common to the plasmon surface wave with  $\text{Re } \epsilon_2 < -1$  and the complex surface wave with  $\text{Re } \epsilon_2 > 1$  and  $\text{Im } \epsilon_2 > 0$ , there exist important differences between them. At first, the plasmon wave is linked with the electron plasma frequencies in metals, while the complex surface waves are due to the absorption losses in dielectrics. Second, the real part of the normalized propagation constant for the plasmon surface wave is larger than 1 and thus even for lossless metals the field is decaying exponentially away from the interface. The corresponding real part of  $k_x/k_0$  for the complex surface wave is less than 1; thus the losses are vital for the existence of such a wave. Otherwise (for lossless dielectrics), the solution for  $k_x/k_0$  represented by Eq. (4) is not a zero of the denominator of the Fresnel coefficients, but rather a zero of the numerator of the reflection coefficient; i.e., it corresponds to the Brewster angle of incidence. The transformation from a pole into a zero is because there exists a cut in the complex  $k_x$  plane, which is required to determine the choice of the sign of the roots in Eq. (2). When the solution given by Eq. (4) crosses the real  $k_x$  axis for values of  $\text{Re } k_x/k_0 < 1$ , the sign of  $k_{1,y}$  changes and this transforms the denominator, given in the left-hand side of Eq. (1) into the numerator of the corresponding reflection coefficient:

$$\epsilon_1/k_{1,y} + \epsilon_2/k_{2,y} \rightarrow -\epsilon_1/k_{1,y} + \epsilon_2/k_{2,y}; \quad (5)$$

i.e., the surface wave is transformed into Brewster's phenomenon.<sup>9</sup>

These considerations are illustrated in Fig. 1, which represents the trajectory of  $k_x/k_0$  as given by Eq. (4) in the complex plane, when the relative permittivity of the substrate is varied between metal and lossy dielectric and then to lossless dielectric. While in nature there is no such diversity of different materials, numerical experiments make it possible to gradually change the real and imaginary part of the permittiv-

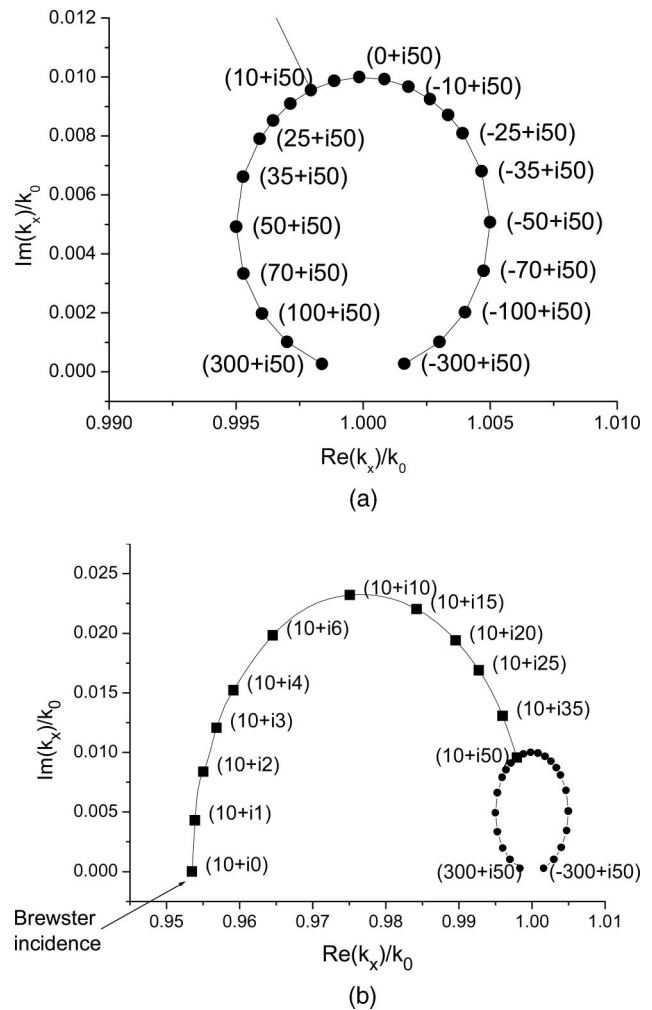


Fig. 1. Trajectory of the normalized propagation constant (i.e., effective index) of the surface wave, obtained as the root of Eq. (1), in the complex  $k$  plane when the dielectric permittivity of the substrate varies from highly conducting metal to (a) lossy dielectric case and to (b) lossless dielectric. Plane interface and vacuum as cladding.

ity to visualize the links between the three different phenomena: plasmon- and complex-type surface waves and Brewster angle of incidence. Figure 1(a) presents the trajectory of  $k_x/k_0$  when the real part of  $\epsilon_2$  is varied from  $-300$  to  $300$ , preserving its imaginary part fixed. One can observe that, when  $\text{Re } \epsilon_2 < 0$ , then  $\text{Re } k_x/k_0 > 1$  and vice versa. The second curve in Fig. 1(b) is obtained by fixing the real part of  $\epsilon_2$  and reducing its imaginary part to observe the transition from metals to lossless dielectrics. This part of the trajectory of  $k_x/k_0$  demonstrates the link between the surface wave types of solutions and the Brewster's incidence. When the imaginary part of  $\epsilon_2$  is gradually reduced, the value of  $k_x/k_0$  moves toward the Brewster incidence, obtained when  $\epsilon_2$  becomes real. This link has been known for a long time,<sup>10</sup> but it is useful to present it because it illustrates quite well the unified nature of different optical phenomena. The main aim of this paper is to show the common features and the differences between the two parts of the curve in

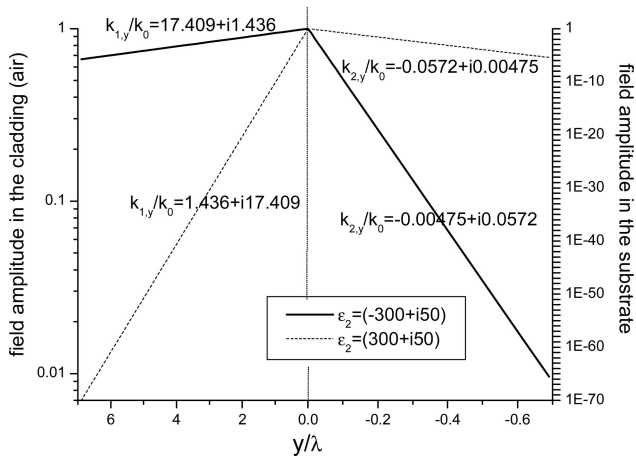


Fig. 2. In-depth decay constants inside the substrate and the cladding for the plasmon surface wave (solid lines) and complex-type surface wave (dashed lines).

Fig. 1(a), with  $\text{Re } k_x/k_0$  being larger or smaller than 1. Figure 2 presents the decay of the field intensity when going away from the interface, positioned at  $y = 0$ . The two surface waves existing, for  $\text{Re } \epsilon_2$  having opposite signs, exhibit quite different behaviors in the cladding and the substrate. The plasmon surface wave (solid curve), decreases quite rapidly inside the

metal (as could be expected inside a highly conducting metal), while decreasing less rapidly inside the cladding. This can be expected when taking into account that, for a perfectly conducting metal, the surface plasmon wave represents a plane wave propagating in vacuum in a direction parallel to the interface, and thus its amplitude is not decreasing when  $y \rightarrow \infty$ .

On the contrary, the decrease of the complex surface wave in the substrate is due to the dielectric losses, and its field extends at a much greater distance, when compared with the plasmon wave. However, its decay in the cladding is much more rapid.

### 3. Total Absorption of Light by Surface Relief Gratings due to Surface Plasmon or Complex Surface Wave Excitation

Total absorption of light by metallic gratings due to surface plasmon excitation was discovered more than 20 years ago<sup>9</sup> for sinusoidal gratings. Figure 3(a) represents the wavelength–groove-depth dependence of the zeroth reflected order of a lamellar grating ruled in a substrate having  $\epsilon_2 = -300 + i50$  illuminated under normal incidence in TM polarization. Several metals have permittivity in the near infrared close to this value. For example, at a wavelength of  $2 \mu\text{m}$ , aluminum permittivity is equal to  $-267 + i77$ . The

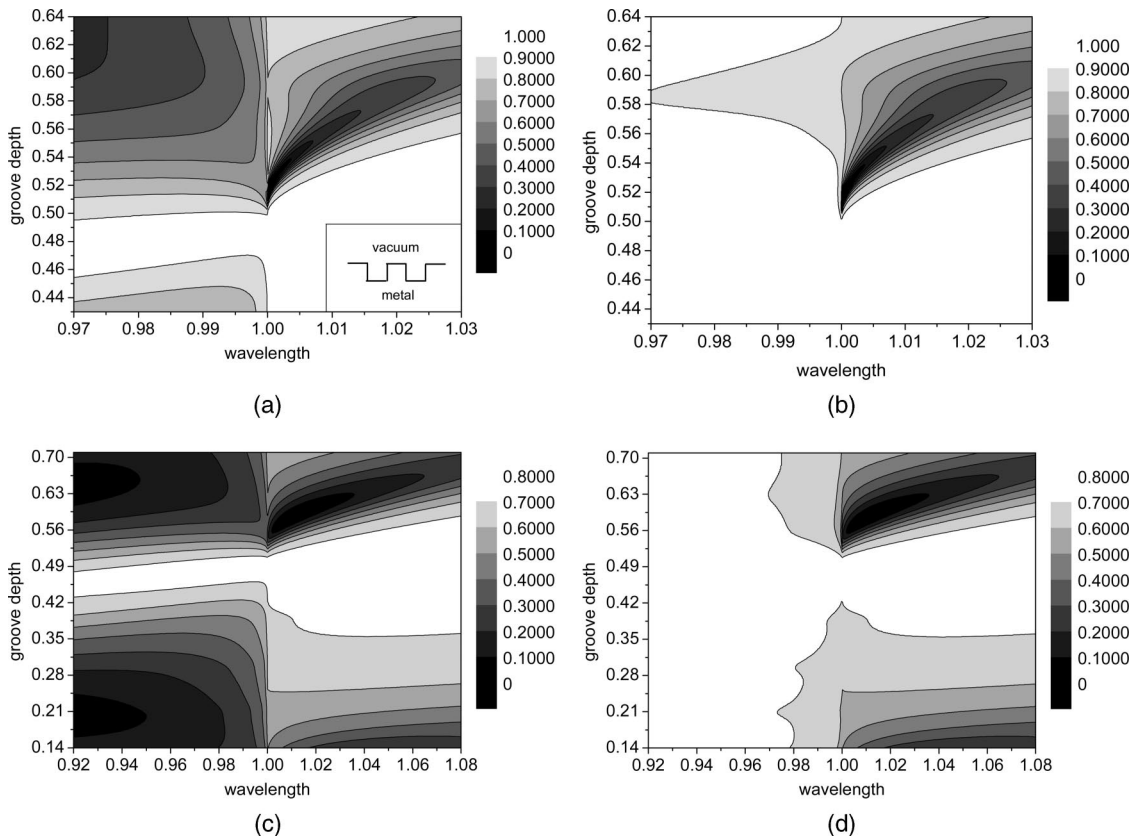


Fig. 3. (a), (c) Map of the zeroth-order efficiency and (b), (d) the total reflectivity in normal incidence (TM polarization) as a function of wavelength and groove depth for a lamellar grating having a period of  $d = 1$  and made of metal with (a), (b)  $\epsilon_2 = -300 + i50$  and (c), (d) lossy dielectric with  $\epsilon_2 = 300 + i50$ . The substrate is filled with the same material as the lamellae and the groove width is equal to the lamella width. Inset of (a) represents the grating geometry.

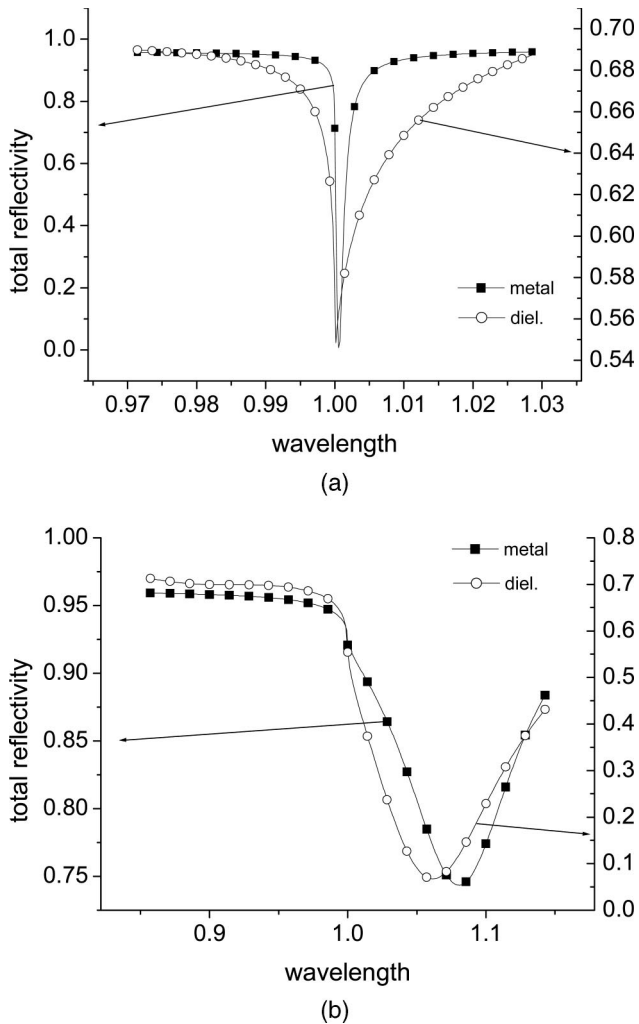


Fig. 4. Spectral dependence of reflectivity in normal incidence in the vicinity of the absorption dips of Fig. 3, metallic grating on the left and dielectric on the right. Groove depth: (a)  $h = 0.524d$ , (b)  $h = 0.57d$ .

groove period  $d$  is equal to 1 (arbitrary unit) and the groove width is half the period. As one can observe, for groove depth values close to 0.51, there is a minimum in the efficiency for wavelengths slightly greater than the period. The reflection minimum is even more pronounced when one looks at the total diffracted energy (the sum of orders 0 and  $\pm 1$ ) in Fig. 3(b). As can be observed, at a certain groove depth (0.524) and wavelength (1.001) the incident light is totally absorbed inside the substrate, although the corresponding plane interface reflects more than 98% of the incident energy.

The next study concerns a lossy dielectric substrate with  $\epsilon_2 = 300 + i50$ . Such values can be of interest in the terahertz region, where, for example,  $\text{SrTiO}_3$  has a relative permittivity equal to  $370 + i40$  (Ref. 7) at a frequency of 0.5 THz. The reflectivity of the plane substrate of such a material exceeds 79%, but when a grating is ruled on its surface, one can also obtain an almost total absorption of light, similar to the metallic case [Figs. 3(c) and 3(d)]. The reason is that the

propagation constant of the complex surface wave is only slightly different from the propagation constant of the surface plasmon, as found in Fig. 1(a). It is necessary to change slightly the groove depth, when compared with the metallic grating and, as observed in Fig. 3(d), a dielectric grating having a groove depth around 0.57 times the period can absorb almost totally the incident light.

Because the difference in the propagation constants of the two types of surface wave is practically insignificant, for the same groove parameters (but slightly different groove depth, as obtained from Fig. 3) the position and the width of the resonant anomalies are almost identical for the metallic and the dielectric gratings, as shown in Fig. 4, which represents a slice of Figs. 3(c) and 3(d) along a constant groove-depth value  $h$  and zoom in the vicinity of absorption dips. Figure 4(a) corresponds to a groove depth required for maximum absorption by the metallic grating, while Fig. 4(b) presents the reflectivity for the groove depth optimal for maximum absorption by the corresponding dielectric grating.

#### 4. Influence of Surface Waves in Transmission

As already mentioned in Section 1, resonance anomalies play an important role in enhanced transmission through otherwise highly absorbing layers. A comparative study of transmission properties of a rectangular-rod grating made of metallic or lossy dielectric material is presented in Figs. 5 and 6. The substrate now is vacuum and the groove width is taken to be much smaller, equal to 0.0285 times the groove period. Although the slits are quite narrow, it is well known that the transmission of metallic gratings can be quite high in TM polarization<sup>10</sup> due to the existence of a TEM mode inside the hollow metallic waveguide formed by the groove walls, a mode that has no cutoff and can always propagate, whatever the slits width may be.

Figures 5(a) and 5(b) represent the transmitted zeroth-order efficiency as a function of the grating thickness and the wavelength for the metallic and the lossy dielectric grating, respectively. A sharp anomaly is found in the vicinity of the surface wave excitation ( $\lambda/d \approx 1$ ) in the two cases. Fabry-Perot resonances are well visible for the metallic grating, and a gradual decrease of transmission with the groove depth is observed, but the decay is much more rapid for the dielectric grating, as illustrated in Fig. 6, contrary to the tendency found in Fig. 2 for plane layers. This peculiarity of the grating case is because the TEM mode inside the slits for the lossy dielectric grating has a field that penetrates much more inside the dielectric lamellae than the TEM modal field inside the metallic lamellae, as found in Fig. 2. Thus the losses of the TEM mode in the dielectric slits are much greater than the losses in the metallic slits, and the decay with the groove depth is much more rapid for the dielectric grating. To prove these considerations, Table 1 presents the normalized constants of propagation of the TEM mode inside a hollow waveguide with walls made of the corresponding metal or



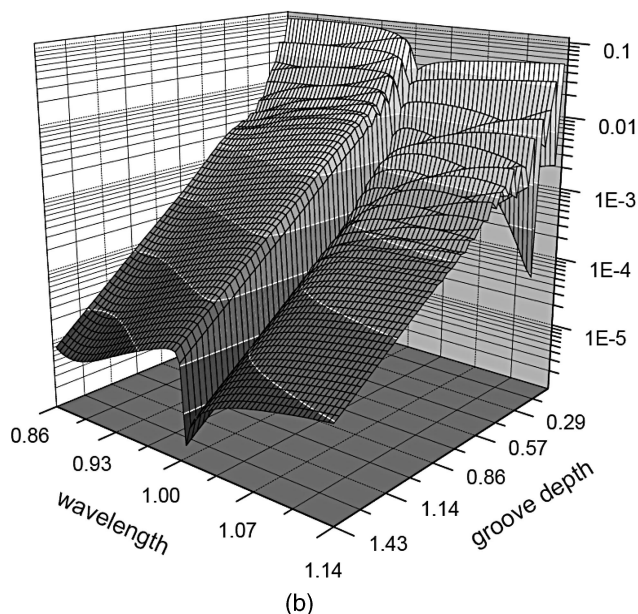
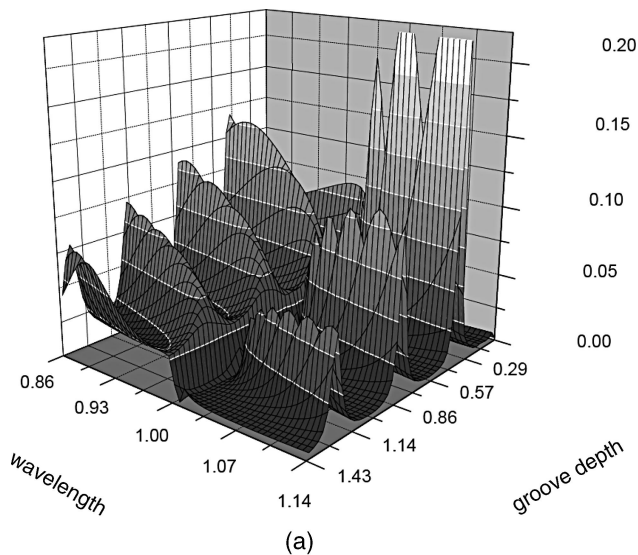


Fig. 5. Transmission through a (a) rectangular-rod metallic and (b) dielectric grating having a period of  $d = 1$ , groove width equal to  $0.0285d$  in normally incident TM polarized light as a function of the wavelength and groove depth (grating thickness). Vacuum in the cladding, the substrate, and the grooves.

lossy dielectric, for both cases of a single isolated slit and periodically arranged slits. The values are slightly different due to the coupling between the modes inside the slits when a grating is considered instead of an isolated slit, but the difference is small and for both uncoupled or coupled slits the imaginary part of the TEM mode for a lossy dielectric material is 15 to 20 times larger than for the metal, which explains the difference in behavior between the two types of material, as observed in Figs. 5 and 6.

### 5. Subwavelength Hole Arrays

The main difference between holes and slits comes from the existence of transverse [TEM (Ref. 11)] guided

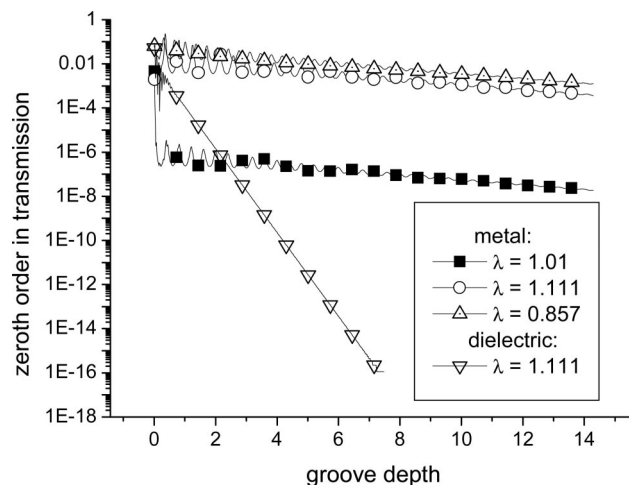


Fig. 6. Dependence of the zeroth transmitted order on the grating thickness for several wavelength values for a metallic and a lossy dielectric grating in the vicinity of the resonance anomaly in Fig. 5.

modes in slits that do not have cutoff wavelengths while the modes inside a hole have such a cutoff. This cutoff makes the two- and three-dimensional structures behave in considerably different ways.<sup>12</sup> For the periodic array of subwavelength holes pierced inside a metallic screen, we expect to have modes with a large imaginary part of the propagating constant. The transmission by the structure is usually governed by the guided mode with the smallest imaginary part. For the dielectric structure the situation is different, the transmission by the layer itself (without any hole) is not negligible as it is for the metallic one, so we expect to find a transmission governed by a propagation constant with the imaginary part much lower.

Figures 7 and 8 show the transmission for a bi-periodic array of square holes with a period  $d$  equal to 1 (arbitrary unit); the edge  $w$  of the square holes is  $0.3d$ , the thickness of the layer  $e$  varies, and the array is lying in vacuum. The permittivity  $\epsilon$  of the layer is  $-300 + i50$  (Fig. 7) or  $300 + i50$  (Fig. 8). The transmission by the metallic structure is consistent with the behavior usually found for subwavelength holes. We can observe an enhanced transmission when the surface plasmon is excited for a wavelength slightly greater than one, which corresponds to the conditions of excitation of a surface plasmon (with a real part of the propagation constant  $k_x/k_0 \approx 1$ , as obtained from Fig. 1) on the metal–vacuum interface with the help of the periodicity of the hole array. These phase conditions at normal incidence fix the position of the anomaly due to a surface wave excitation having

Table 1. Normalized Propagation Constants of the TEM Modes<sup>a</sup>

$\epsilon_2$	Isolated Slit	Lamellar Grooves
$-300 + i50$	$1.3157 + i0.02317$	$1.29 + i0.0227$
$300 + i50$	$1.0827 + i0.3354$	$1.051 + i0.398$

<sup>a</sup>Inside isolated slits or slits arranged periodically with walls made of metallic or lossy dielectric material.

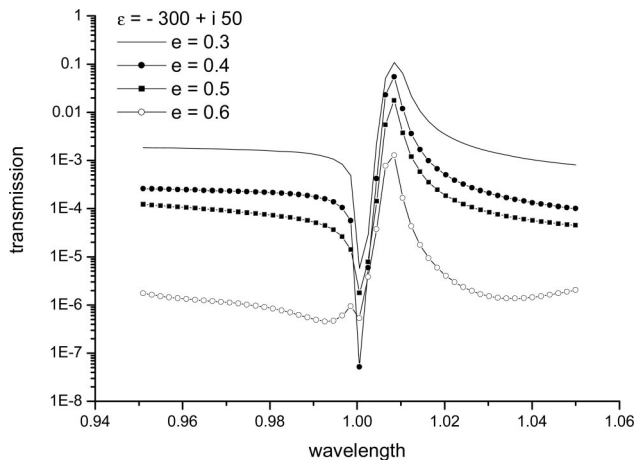


Fig. 7. Transmission for a biperiodic array of square holes in a metallic layer with  $\varepsilon = -300 + i50$  and a period  $d$  equal to 1 (arbitrary unit); the edge of the square holes is  $w = 0.3d$ , the thickness of the layer  $e$  varies, and the array is lying in vacuum.

$k_x/k_0 \approx 1$ , which has to appear close to  $\lambda/d = 1$ . And indeed, such an anomaly is observed in both Figs. 7 and 8. A maximum transmission of about 0.1 has then been obtained in Fig. 7 (for  $e = 0.3$ ), and we have checked that the decay of the transmission with the thickness is exponential. This decay has been found to be driven by the guided mode in the holes with a normalized propagation constant equal to  $0.015 + i1.23$ , having an imaginary part much smaller than the imaginary part of the refractive index of the metal  $n_m'' = 17.38$ , but much larger than in the monodimensional case (Table 1).

When a lossy dielectric structure is considered, the transmission spectra can also present enhancement (for example, for a thickness of 0.4) but not necessarily ( $e = 0.3, e \geq 1$ ), and when the peak is distinguishable it is always much less pronounced than for its metallic counterpart. Moreover, to reach a regime

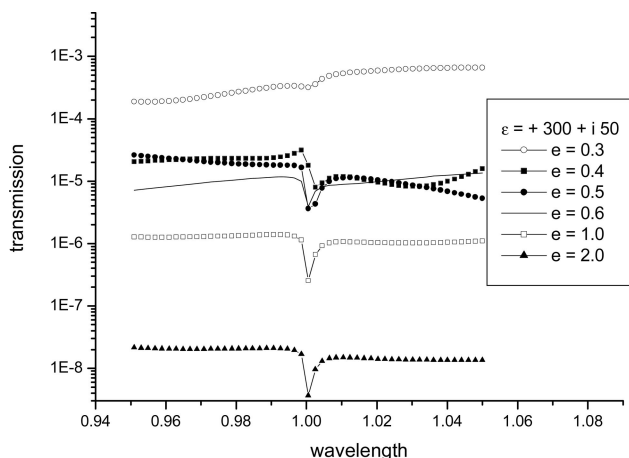


Fig. 8. Transmission for a biperiodic array of square holes in a lossy dielectric layer with  $\varepsilon = 300 + i50$  and a period  $d$  equal to 1 (arbitrary unit), the edge of the square holes is  $w = 0.3d$ , the thickness of the layer  $e$  varies, and the array is lying in vacuum.

with exponential decay we had to considerably increase the thickness. Indeed, it should be noticed that the transmission for values of the thickness in the range of  $0.4d$  to  $0.6d$  has values having the same order of magnitude. It can be understood as a result of the competition of several modes for the lower values of the thickness. For the smallest thickness ( $e = 0.3$ ), the tunneling through the layer is still quite strong,  $\sim 3 \cdot 10^{-4}$ , and predominates over the other effects. When the thickness has a sufficient value, the decay is found to be dominated by the mode whose normalized propagation constant is  $3.24 + i0.344$ . Note that the imaginary part is almost the same as in the monodimensional case (Table 1) and four times smaller than the imaginary part of the refractive index of the unpierced layer  $n_d'' = 1.4384$ .

## 6. Conclusion

Lossy dielectric and metallic surfaces and layers may both support surface waves, called most often, respectively, polaritons and plasmons. However, these surface waves have quite different properties. The plasmon field decreases quite rapidly in the metal depth, while extending much farther in the cladding (vacuum or lossless dielectric). Although polaritons can be characterized by almost identical values of their propagation constant, they behave in the opposite way, extending much deeper in the lossy dielectric than in the other media (low-index lossless dielectric or vacuum). This difference can be important in nonlinear optics, where the larger the penetration of the electric field inside optically nonlinear media, the stronger the nonlinear effect, in general. When considering one- or two-dimensional periodic structures made of such materials, the transmission enhancement due to the excitation of surface plasmons or polaritons is much more pronounced in the metallic structure, because of the smaller losses, which are due to the smaller penetration of the field inside the lossy medium.

The support of the European Community funded project PHOREMOST (FP6/2003/IST/2-511616) is gratefully acknowledged.

## References

1. R. W. Wood, "On a remarkable case of uneven distribution of light in a diffraction grating spectrum," *Philos. Mag.* **4**, 396–402 (1902).
2. T. W. Ebbesen, H. J. Lezec, H. F. Ghaemi, T. Thio, and P. A. Wolff, "Extraordinary optical transmission through subwavelength hole arrays," *Nature* **391**, 667–669 (1998).
3. M. J. Levene, J. Korlach, S. W. Turner, M. Foquet, H. G. Craighead, and W. W. Webb, "Zero-mode waveguides for single-molecule analysis at high concentrations," *Science* **299**, 682–686 (2003).
4. E. Popov, S. Enoch, G. Tayeb, M. Nevère, B. Gralak, and N. Bonod, "Enhanced transmission due to non-plasmon resonances in one and two dimensional gratings," *Appl. Opt.* **43**, 999–1008 (2004).
5. E. Popov, L. Mashev, and D. Maystre, "Theoretical study of the anomalies of coated dielectric gratings," *Opt. Acta* **33**, 607 (1986).

6. F. Marquier, K. Joulain, and J.-J. Greffet, "Resonant infrared transmission through SiC films," *Opt. Lett.* **29**, 2178–2180 (2004).
7. F. Miyamaru, M. Tanaka, and M. Hangyo, "Resonant electromagnetic wave transmission through strontium titanate hole arrays without surface plasmon polaritons," *Phys. Rev. B* **74**, 115–117 (2006).
8. M. Nevière and E. Popov, *Light Propagation in Periodic Media: Diffraction Theory and Design* (Marcel Dekker, 2003).
9. M. C. Hutley and D. Maystre, "The total absorption of light by a diffraction grating," *Opt. Commun.* **19**, 431–436 (1976).
10. R. Petit, ed., *Electromagnetic Theory of Gratings* (Springer, 1980), Chap. 5.
11. A. Snyder and J. Love, ed., *Optical Waveguide Theory* (Chapman & Hall, 1983).
12. E. Popov, M. Nevière, S. Enoch, and R. Reinisch, "Theory of light transmission through subwavelength periodic hole arrays," *Phys. Rev. B* **62**, 16100–16108 (2000).